THE JOURNAL OF BIOLOGICAL CHEMISTRY VOL. 285, NO. 16, pp. 12390–12404, April 16, 2010

Free Oligosaccharides to Monitor Glycoprotein Endoplasmic Reticulum-associated Degradation in *Saccharomyces cerevisiae*[*] [S]

Received for publication, November 3, 2009, and in revised form, February 8, 2010 Published, JBC Papers in Press, February 11, 2010, DOI 10.1074/jbc.M109.082081

Hiroto Hirayama[‡], Junichi Seino[‡], Toshihiko Kitajima[§], Yoshifumi Jigami[§], and Tadashi Suzuki[‡¶1]

From the [‡]Glycometabolome Team, Systems Glycobiology Research Group, RIKEN Advanced Science Institute, 2-1 Hirosawa, Wako, Saitama 351-0198, Japan, the [§]Research Center for Medical Glycoscience, National Institute of Advanced Industrial Science and Technology, Central 6, 1-1-1 Higashi, Tsukuba, Ibaraki 305-8566, Japan, and [¶]Core Research for Evolutionary Science and Technology, Japan Science and Technology Agency, 4-1-8 Honcho, Kawaguchi, Saitama 332-0012, Japan

In eukaryotic cells, *N*-glycosylation has been recognized as one of the most common and functionally important co- or post-translational modifications of proteins. "Free" forms of *N*-glycans accumulate in the cytosol of mammalian cells, but the precise mechanism for their formation and degradation remains unknown. Here, we report a method for the isolation of yeast free oligosaccharides (fOSs) using endo-β-1,6-glucanase digestion. fOSs were undetectable in cells lacking *PNG1*, coding the cytoplasmic peptide:*N*-glycanase gene, suggesting that almost all fOSs were formed from misfolded glycoproteins by Png1p. Structural studies revealed that the most abundant fOS was M8B, which is not recognized well by the endoplasmic reticulum-associated degradation (ERAD)-related lectin, Yos9p. In addition, we provide evidence that some of the ERAD substrates reached the Golgi apparatus prior to retrotranslocation to the cytosol. *N*-Glycan structures on misfolded glycoproteins in cells lacking the cytosol/vacuole α-mannosidase, Ams1p, was still quite diverse, indicating that processing of *N*-glycans on misfolded glycoproteins was more complex than currently envisaged. Under ER stress, an increase in fOSs was observed, whereas levels of M7C, a key glycan structure recognized by Yos9p, were unchanged. Our method can thus provide valuable information on the molecular mechanism of glycoprotein ERAD in *Saccharomyces cerevisiae.*

In eukaryotic cells, *N*-glycosylation takes place in the endoplasmic reticulum (ER).[2] *N*-Linked glycans are transferred to Asn-X-Ser/Thr (where *X* can represent any amino acid except proline) of nascent polypeptide chains by oligosaccharyl transferase using, in most cases, dolicholpyrophosphate-linked $Glc_3Man_9GlcNAc_2$ as a donor substrate (1, 2). *N*-Glycans contribute to the physicochemical properties of core proteins, such as solubility and heat stability, as well as their physiological properties, such as the bioactivity or intra- and intercellular distribution (3). In addition, recent studies have shown that *N*-glycans play a pivotal role in the correct folding or degradation of proteins. The former process is called ER quality control, whereas the latter is called ER-associated degradation (ERAD) (4).

In ER quality control, the $Glc_3Man_9GlcNAc_2$ form of the donor glycan, linked covalently to nascent proteins, is rapidly trimmed by enzymes glucosidases I and II and, in some cases, ER α-mannosidase I, converting it to G1M8–9GN2. Lectin-like molecular chaperones, calnexin/calreticulin, are known to interact with the monoglucosylated glycans and promote the correct folding of nascent glycoproteins (5–8). In higher eukaryotes, calnexin/calreticulin and UDP-glucose:glycoprotein glucosyltransferase assist folding of *N*-glycoproteins (4, 9). Removal of the remaining glucose by glucosidase II frees the native folded glycoprotein from the lectins. On the other hand, in the ERAD system, *N*-glycans on misfolded glycoproteins are further trimmed of α-1,2-linked terminal mannose residues by ER α-mannosidase I as well as EDEMs (ER-degradation enhancing α-mannosidase-like proteins; Mns1p and Htm1/Mnl1p in yeast, respectively), to generate the M7C form of the glycan (10–12) (see Table 3 for the detailed structure). It is known that the M7C glycan was then recognized by a degradation sensor lectin, Yos9p, and that this interaction facilitates its ERAD-dependent degradation (13–17). The retrotranslocated misfolded glycoproteins are deglycosylated by a cytosolic peptide:*N*-glycanase (PNGase) (18, 19). Deglycosylation by PNGase is known to increase the degradation efficiency of certain ERAD substrates (20, 21), and the activity of PNGase has been suggested to play a role in the antigen presentation process in mammalian cells (22–25). It is therefore well established that cells dictate subtle structural differences in the *N*-glycans on nascent glycoproteins to facilitate their folding or degradation. However, the fate of released *N*-glycans from misfolded glycoproteins, called free oligosaccharides (fOSs), are poorly understood.

It has been reported that fOSs can be released not only from misfolded glycoproteins but also from dolicholpyrophosphate-

[*] This work was supported in part by the Global Center of Excellence Program, the RIKEN President's Discretionary Fund (Strategic Programs for R & D), and a grant-in-aid for scientific research from the Ministry of Education, Culture, Sports, Science, and Technology of Japan (to T. S.).

[S] The on-line version of this article (available at http://www.jbc.org) contains supplemental Table S1 and Figs. S1–S3.

[1] To whom correspondence should be addressed. Tel.: 81-48-467-9628; Fax: 81-48-467-9626; E-mail: tsuzuki_gm@riken.jp.

[2] The abbreviations used are: ER, endoplasmic reticulum; Dol-PP-OS, dolichol-pyrophosphate-linked oligosaccharide; DTT, dithiothreitol; ERAD, endoplasmic reticulum-associated degradation; fOS, free oligosaccharide; GU, glucose unit; HPLC, high performance liquid chromatography; JB, jack bean; MALDI-TOF, matrix-assisted laser desorption ionization time-of-flight; MS, mass spectrometry; PA, pyridylamino; PNGase, peptide:*N*-glycanase; Tm, tunicamycin; UPR, unfolded protein response; HA, hemagglutinin.

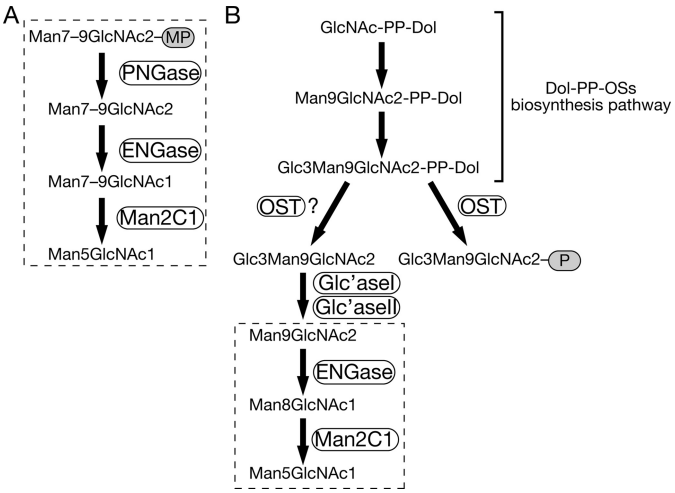

FIGURE 1. **Two generation and processing pathways for fOSs in mammalian cells.** *A*, PNGase-dependent fOS generation and processing pathway. *B*, fOSs derived from Dol-PP-OS-processing pathways. These fOSs are further processed by cytosol-localized hydorolases, endo-β-*N*-acetylglucosaminidase, and α-mannosidase. *P* and *MP*, protein and misfolded protein, respectively. Regions *circled* by a *dotted line* indicate processing reactions occurring in the cytosol.

linked oligosaccharides (Dol-PP-OSs), as depicted in Fig. 1, *A* and *B*, respectively (18, 19, 26, 27). Free oligosaccharides generated from Dol-PP-OSs by an unclarified mechanism in the ER lumen are exported from the ER to the cytosol in an ATP-dependent manner (28, 29). In vertebrates, fOSs in the cytosol are further trimmed by two enzymes, endo-β-*N*-acetylglucosaminidase and α-mannosidase (30–32). Consequently, these organisms contain a great variety of GN2 (bearing di-*N*-acetylchitobiose at their reducing termini) and GN1 (bearing a single GlcNAc at their reducing termini) forms of fOSs in the cytosol (33–35), which are then transported to the lysosomes by a putative transporter on the lysosomal membranes (36, 37). The presence of fOSs, as well as glycan processing enzymes, has also been shown in *Caenorhabditis elegans* (38–40), but the detailed molecular mechanism of fOS formation/degradation remains unknown. In yeast, previous studies reported the occurrence of fOSs in *Saccharomyces cerevisiae* (41, 42) that were degraded mainly by a cytosol/vacuole α-mannosidase, Ams1p (42). However, detailed structural determination of fOSs still remains to be determined.

To identify the precise structures of fOSs from yeast, we used a method previously applied to analyze them in other organisms (33, 38), *i.e.* pyridylamination (PA) of oligosaccharides followed by HPLC analysis. However, we found that most of the PA-labeled oligosaccharides were not derived from fOSs but from β-1,6-glucans. We therefore treated the PA-oligosaccharide fractions with purified endo-1,6-β-glucanase to successfully isolate the fOSs. By HPLC analysis of the PA-labeled fOSs, we found that yeast cells have a great variety of the GN2 form of fOSs, ranging from Hex_5 to $Hex_{12}HexNAc_2$, with various isomeric structures. To our surprise, almost all fOSs in yeast cells were found to be generated from misfolded glycoproteins by Png1p because we did not detect any fOSs in *png1*Δ cells under our experimental conditions. If Ams1p was deleted, fOSs smaller than $Man_7GlcNAc_2$ disappeared, suggesting that Ams1p is the sole enzyme demannosylating the fOSs in the cytosol. A mutant having a defect of Cvt (cytosol-to-vacuole targeting), a pathway required for Ams1p to target to the vacuole, resulted in more pronounced demannosylation of fOSs, clearly indicating that Ams1p can act on fOSs in the cytosol. We further showed that the M8B structure and several *N*-glycan structures were modified by Golgi-resident mannosyltransferases, and the amount of these Golgi-modified glycans was significantly increased upon DTT-mediated ER stress. In sharp contrast, however, the amount of M7C, presumably a key structure for glycoprotein ERAD substrates to be recognized by Yos9p, did not change. This newly established method to identify fOSs in yeast will be invaluable to provide deeper insight into the mechanism of the glycoprotein ERAD pathway.

TABLE 1
Yeast strains used in this study

Strain	Genotype	Source[a]
BY4741	*MAT***a** *his3Δ1 leu2Δ0 met15Δ0 ura3Δ0*	ATCC
*png1*Δ	*MAT***a** *png1*Δ::*kanMX6* BY4741	SDP
*ams1*Δ	*MAT***a** *ams1*Δ::*kanMX6* BY4741	SDP
*atg19*Δ	*MAT***a** *atg19*Δ::*kanMX6*	SDP
YME2028	*MAT***a** *AMS1*::*AMS1-3xHA-His3MX6* BY4741	This study

[a] ATCC, American Type Culture Collection; SDP, *Saccharomyces* Deletion Project- (available at the Stanford Web site).

EXPERIMENTAL PROCEDURES

Strains, Growth Conditions, and Gene Disruption—We used a BL21(DE3) strain of *Escherichia coli* (Novagen, Madison, WI) to produce His_6-tagged endo-1,6-β-glucanase (His_6-Neg1). The yeast strains used in this study are listed in Table 1. Integration of a DNA fragment encoding 3× HA epitope at the 3′-end of the chromosomal *AMS1* locus was performed by the one-step PCR method (43). Yeast cells were grown in YPD medium (1% yeast extract, 2% polypeptone, 2% glucose).

Construction of His_6-Neg1 Expression Vector—The mature *neg1* coding region from *Neurospora crassa*, excluding the secretory signal sequence, was PCR-amplified using genomic DNA of *N. crassa* strain 74-OR23-1A as a template, primers NheI-Nc-mneg1-fwd (5′-AAAAGCTAGCGCGATCCAACCCCAAGCCTATG-3′) and XhoI-Nc-neg1-rvs (5′-AAAACTCGAGTTACGCCCCTGCAGCCGGCAAAAC-3′), and Phusion Hot Start DNA polymerase (FINNZYMES Inc., Epoo, Finland). The underlined bases in the primer sequences indicate NheI and XhoI sites, respectively. The amplified 1412-base pair fragment, which excluded the signal sequence (44), was digested with NheI and XhoI and then purified. The purified fragment was ligated into the equivalent site of the vector pET-28a (+) (Novagen) to generate pHI-NCNEG1 (His_6-Neg1 expression vector).

Endo-1,6-β-glucanase (Neg1) Expression in E. coli and Purification—E. coli BL21(DE3) cells harboring the His_6-tagged Neg1 expression plasmid were grown at 30 °C in 1 liter of LB broth containing kanamycin (50 μg/ml) until the A_{600} reached 0.4. After the addition of isopropyl-1-thio-β-D-galactoside to a final concentration of 0.05 mM, the culture was incubated with agitation (160 rpm) at 20 °C for 14 h.

The cells were harvested and lysed using 30 ml of BugBuster® (Novagen) containing Complete™ protease inhibitor mixture (Roche Applied Science) at 25 °C for 20 min. The cell lysate was centrifuged at 100,000 × *g* for 20 min at 4 °C to remove the

insoluble fraction, and then the supernatant was applied to 5 ml of nickel-Sepharose resin (GE Healthcare) prewashed with equilibration buffer (20 mM Tris-HCl (pH 8.0), 300 mM NaCl). The column was washed with 25 ml of equilibration buffer, 25 ml of washing buffer 1 (equilibration buffer containing 25 mM imidazole), and 25 ml of washing buffer 2 (equilibration buffer containing 50 mM imidazole). Finally, elution of His_6-Neg1 was carried out with equilibration buffer containing 500 mM imidazole. The eluted fraction was dialyzed with 20 mM Tris-HCl (pH 8.0) and then concentrated to 1.3 mg/ml using Amicon Ultra-15 (30,000 molecular weight cut-off; Millipore, Billerica, MA). Protein concentrations were measured by the BCA method (Thermo Scientific, Waltham, MA), according to the manufacturer's instructions, using bovine serum albumin as a standard.

Endo-1,6-β-glucanase Assay—An *in vitro* assay for endo-1,6-β-glucanase was performed as follows. The reaction mixture contained 100 mM sodium acetate buffer (pH 5.0), 30 pmol of PA-gentiohexaose, and His_6-Neg1 in a total volume of 20 μl. The mixtures were incubated at 30 °C for 15 min, and the reaction was terminated by adding 100 μl of 100% ethanol. Protein precipitate was removed by centrifugation at room temperature at 20,000 × *g* for 5 min. Supernatant was dried up, resuspended in water, and analyzed by HPLC. One unit was defined as the amount of enzyme that catalyzes hydrolysis of 1 nmol of PA-gentiohexaose/min.

Preparation of PA-oligosaccharide Standards—The following standards of PA-oligosaccharides and PA-monosaccharides were purchased from TaKaRa (Kyoto, Japan): PA-Glc, PA-ManNAc, PA-GlcNAc, PA-Man, PA-M5A, PA-M6B, PA-M7A, PA-M7C, PA-M8A, PA-M8B, PA-M8C, PA-M9A, and PA-glucose oligomer. PA-G1M9A was prepared as described previously (45). G1M7-PA and G1M5-PA were prepared by the digestion of G1M9-PA with *Aspergillus saitoi* α-1,2-mannosidase and jack bean α-mannosidase, respectively (Seikagaku Corp., Tokyo, Japan). PA-gentiohexaose was prepared by PA labeling of gentiohexaose (Seikagaku Corp.). The structures of these standards were confirmed by matrix-assisted laser desorption ionization time-of-flight (MALDI-TOF) MS.

PA-labeled yeast specific *N*-glycans, modified by Och1p, were synthesized by enzymatic reactions using purified recombinant Och1p protein expressed by the methylotrophic yeast *Pichia pastoris* as a secreted protein (46). The reaction mixtures contained 50 mM Tris-HCl (pH 7.5), 10 mM $MnCl_2$, 1 mM GDP-mannose, 2 μM pyridylaminated oligosaccharide acceptors (PA-M7A, PA-M7C, PA-M7D, PA-M8A, PA-M8B and PA-M8C), and 60 ng of Och1p in a total volume of 20 μl. Incubation was carried out at 30 °C for 5 min, terminated by boiling for 5 min, and the reaction products were fractionated by size fractionation HPLC.

Extraction of Cytosolic Free Oligosaccharides from Yeast Cells—Yeast cells were inoculated into 5 ml of YPD medium and grown at 30 °C overnight. Saturated cultures were further inoculated into 50 ml of YPD medium and grown at early to mid-logarithm growth phase. Then, 100 A_{600} units of yeast cells were washed twice (all centrifugation steps in this protocol were carried out at 4 °C); resuspended in 500 μl of fOSs extraction buffer containing mannosidase inhibitors (20 mM Tris-HCl (pH 7.5), 10 mM EDTA, 1 mM 1-deoxymannojirimycin (Calbiochem, Darmstadt, Germany), 0.5 mM swainsonine (Calbiochem), and protease inhibitor mixture (Roche Applied Science)); and disrupted with glass beads using Multi-beads Shocker® (Yasui Kikai, Osaka, Japan), according to the manufacturer's protocol. Mannosidase inhibitors were added to prevent degradation of fOSs during sample preparation. After removing cell debris by brief centrifugation, the supernatant was further centrifuged at 100,000 × *g* for 20 min to obtain the cytosolic fraction. 750 μl of 100% ethanol was then added to the supernatant (final concentration, 60%), and the sample was further centrifuged at 20,000 × *g* for 5 min to precipitate proteins. The supernatants, representing the fOSs fraction, were evaporated to dryness, dissolved in water, and applied onto AG1-X2 (resin volume, 500 μl; 200–400 mesh; acetate form) and AG50-X8 (resin volume, 500 μl; 200–400 mesh; H^+ form) (Bio-Rad) columns. Neutral material, including the fOSs (flow-through fractions for both columns), was loaded onto an InertSep GC column (150 mg/3 ml; GL-Science, Tokyo, Japan). The fOS fraction was adsorbed to the column, which was rinsed with 3 ml of water and fOSs were eluted with 2.5 ml of 25% acetonitrile. Finally, the desalted fOS fraction was lyophilized.

Preparation of PA-labeled Oligosaccharides—The preparation of PA-labeled oligosaccharides was carried out as described previously (47) with some modifications. The desalted fOS fractions were pyridylaminated with 20 μl of 2-amino pyridine reagent at 80 °C for 1 h, followed by reduction at 80 °C for 1 h with 20 μl of borane-dimethylamine reagent. After adding 460 μl of acetonitrile into the reaction mixture, excess free PA was removed using a monolithic silica spin column (MonoFas® (GL-Science)). The spin column was initially washed with water and then activated with 600 μl of 100% acetonitrile. The sample solution was loaded onto the spin column. After washing the column three times with 400 μl of 95% acetonitrile, PA-oligosaccharides were eluted from the column with 100 μl of water.

High Performance Liquid Chromatography Analysis—Size fractionation HPLC was carried out using a Shodex NH2P-50 4E column (4.6 × 250 mm; Shodex, Tokyo, Japan) as reported previously (48), with some modifications. The elution was performed using two solvent gradients as follows: eluent A, 93% acetonitrile in 0.3% acetate (pH adjusted to 7.0 with ammonia); eluent B, 20% acetonitrile in 0.3% acetate (pH adjusted to 7.0 with ammonia). The gradient program was set at a flow rate of 0.8 ml/min (expressed as the percentage of solvent B): 0–5 min, isocratic 3%; 5–8 min, 3–33%; 8–40 min, 33–71%. PA-oligosaccharides were detected by measuring fluorescence (excitation wavelength, 310 nm; emission wavelength, 380 nm).

Reversed-phase HPLC was performed using a TSK-gel ODS-80TM column (4.6 × 150 mm; TOSOH, Tokyo, Japan) as described previously (47), with some modifications. The elution conditions were as follows: eluent C, 20 mM ammonium acetate buffer, pH 4.0; eluent D, 20 mM ammonium acetate buffer, pH 4.0, containing 0.5% 1-butanol. The column was equilibrated with eluent C/eluent D (95:5) at a flow rate of 1.0 ml/min. After injecting a sample, the concentration of eluent D was increased linearly from 5 to 75% over 55 min. PA-oligosaccharides were detected by measuring fluorescence (excitation

wavelength, 320 nm; emission wavelength, 400 nm). The glucose unit (GU) of each PA-labeled oligosaccharide was determined as described previously (45).

For PA-monosaccharide analysis, HPLC was performed as described previously (49). Briefly, a flow rate of 0.3 ml/min was used on a TSK-gel Sugar-AXI column (4.6 × 150 mm; TOSOH) with isocratic elution with borate solution (700 mM H_3BO_3-KOH, 10% acetonitrile (pH 9.0)) for 120 min at 65 °C. PA-oligosaccharides were detected by measuring fluorescence (excitation wavelength, 310 nm; emission wavelength, 380 nm).

MALDI-TOF MS Analysis—MALDI-TOF MS analysis of PA-oligosaccharides was performed by AXIMA-CFR (Shimadzu, Kyoto, Japan) using 2,5-dihydroxybenzoic acid (Shimadzu) as a matrix as described previously (31). For desalting of PA-oligosaccharide-containing fractions, we used C18+ carbon NuTip (Hypercrb, Glygen, Columbia, MD) as described previously (31).

Reducing End Analysis of PA-oligosaccharides—Reducing end analysis of PA-oligosaccharides was performed as described previously (49), with some modifications. PA-oligosaccharide was hydrolyzed with 20 μl of 4 M trifluoroacetic acid at 100 °C for 3 h. For re-*N*-acetylation, the lyophilized hydrolysates were resuspended in 4 μl of pyridine, 36 μl of 90% methanol, and 10 μl of acetic anhydride, followed by incubation at 25 °C for 30 min, and the reaction mixtures were evaporated. The PA-monosaccharides obtained were separated by HPLC using a TSK-gel Sugar-AXI column (TOSOH).

Glycosidase Digestions—The digestion of PA-fOSs with jack bean α-mannosidase (40 milliunits) (Seikagaku Corp.) was performed (to cleave α1,2-, α1,3-, and α1,6-linked mannoses in fOSs) by incubation in 20 μl of 10 mM sodium citrate buffer (pH 4.0) for 12 h at 37 °C. *A. saitoi* α-1,2-mannosidase (0.5 milliunits) (Seikagaku Corp.) digestion was performed in 20 μl of 100 mM sodium acetate (pH 5.0) for 12 h at 37 °C. The digestion of PA-fOSs with α-1,6-mannosidase (10 milliunits) or α-1,2,3-mannosidase (60 units), cloned from *Xanthomonas manihotis* and expressed in *Escherichia coli* (New England Biolabs, Beverly, MA), was performed in 20-μl reactions with a buffer supplied by the manufacturer at 37 °C for 12 h.

Reverse Transcription-PCR of HAC1 mRNA—The splicing of *HAC1* was assayed using reverse transcription-PCR as described previously (50). Briefly, *ams1*Δ cells were grown to mid-log phase in YPD medium and treated with/without 2 mM DTT or 2 μg/ml tunicamycin for 90 min. The cells were collected, and total RNA was extracted using the RNeasy minikit (Qiagen, Valencia, CA) according to the manufacturer's instructions. cDNA was generated from 2 μg of total mRNA using the Primescript first strand cDNA synthesis kit (TaKaRa). Uninduced *HAC1* (*HAC1*^{u}), induced *HAC1* (*HAC1*^{i}), and *ACT1* cDNA were amplified by PCR using 50 ng of template cDNA and the primers HAC1-fwd (5′-TACAGGGATTTCCAGAGCACG-3′), HAC1-rvs (5′-TCATGAAGTGATGAAGAAATC-3′), ACT1-fwd (5′-TTTGGATTCCGGTGATGGTG-3′), and ACT1-rvs (5′-TTGTGGTGAACGATAGATGGA-3′). Amplicons were analyzed by electrophoresis on 2% agarose gels.

Protein Extraction and Immunoblot Analysis—Yeast cells were grown to mid-log or stationary phase in YPD medium. Ten A_{600} units of cells were then harvested, washed twice with water, resuspended in 100 μl of TEG buffer (50 mM Tris-HCl (pH 7.5), 100 mM NaCl, 1 mM EDTA, and Complete™ protease inhibitor mixture (Roche Applied Science)), and disrupted with glass beads using a Multi-beads Shocker® (Yasui Kikai). After removal of the cell debris by centrifugation, cell lysates were denatured with sample buffer (125 mM Tris-HCl (pH 6.8), 4% SDS, 20% glycerol, and 3.1% DTT) for 5 min at 98 °C. Samples were separated by SDS-PAGE using 7.5% gels. Proteins were transferred to polyvinylidene difluoride membranes and blocked in TTBS (25 mM Tris-HCl (pH 7.4), 150 mM NaCl, and 0.1% (v/v) Tween 20) containing 0.5% (w/v) skim milk. Blots were incubated with anti-HA mouse monoclonal antibody F-7 (1:1000; Santa Cruz Biotechnology, Inc., (Santa Cruz, CA)), followed by horseradish peroxidase-conjugated sheep anti-mouse IgG antibody (1:4000; GE Healthcare), both in TTBS plus 0.5% skim milk. For the protein-loading control, Pgk1p was detected with anti-Pgk1p mouse monoclonal antibody 22C5 (1:10,000; Invitrogen), followed by horseradish peroxidase-conjugated sheep anti-mouse IgG antibody (1:10,000). Immunoreactive bands were visualized using LAS3000-mini (Fujifilm Co., Tokyo, Japan) with Immobilon Western reagents (Millipore).

RESULTS

Use of Endo-1,6-β-glucanase to Establish the Method for Isolation of Yeast fOSs—Several reports have shown that higher eukaryotic organisms generate fOSs, and extensive studies have revealed that these organisms generate a diverse range of fOS structures, including fOS-GN2 (M6-8GN2) and fOS-GN1 (M2-9GN1 and G1M9GN1), in the cytosol (28, 33–35, 40, 51). It was also reported that *S. cerevisiae* cells generate fOSs and that the predominant structure of fOS is $Man_8GlcNAc_2$ (52). On the other hand, recent studies showed that the M7C form generated by Htm1p was key for the recognition of misfolded glycoprotein substrates for ERAD (11, 14), raising a question about the source of fOSs in yeast. How fOSs are generated, processed, and degraded in yeast remains to be elucidated because of the lack of an established method for the isolation of fOSs. Previous studies of fOSs in yeast relied on metabolic radiolabeling of glycans (41, 52).

We first tried to identify the cytosolic yeast fOSs using the method reported for the isolation of fOSs in higher eukaryotes (*i.e.* the deproteinated, neutral oligosaccharide fraction from the cytosol of wild-type cells was labeled with PA and analyzed by size fractionation HPLC). As shown in Fig. 2*A*, various peaks were observed at the elution position relating to around 3–15 GUs. However, most of these peaks were not susceptible to treatment with jack bean (JB) α-mannosidase (supplemental Fig. S1*A*, *open arrows*). Because yeast cells only have high mannose type *N*-glycans (53–55), the mannosidase-resistant peaks are not likely to be derived from *N*-glycans. Consistent with this idea, reducing end sugar analysis of PA-labeled fOSs in Fraction A (supplemental Fig. S1*A*) revealed that most of the labeled glycans in fraction A had glucose in their reducing termini (supplemental Fig. S1*B*).

In yeast cells, β-1,3- and β-1,6-glucans are the major glycans bearing reducing glucose residues (56). For this reason, we proposed that these α-mannosidase resistance peaks are derived

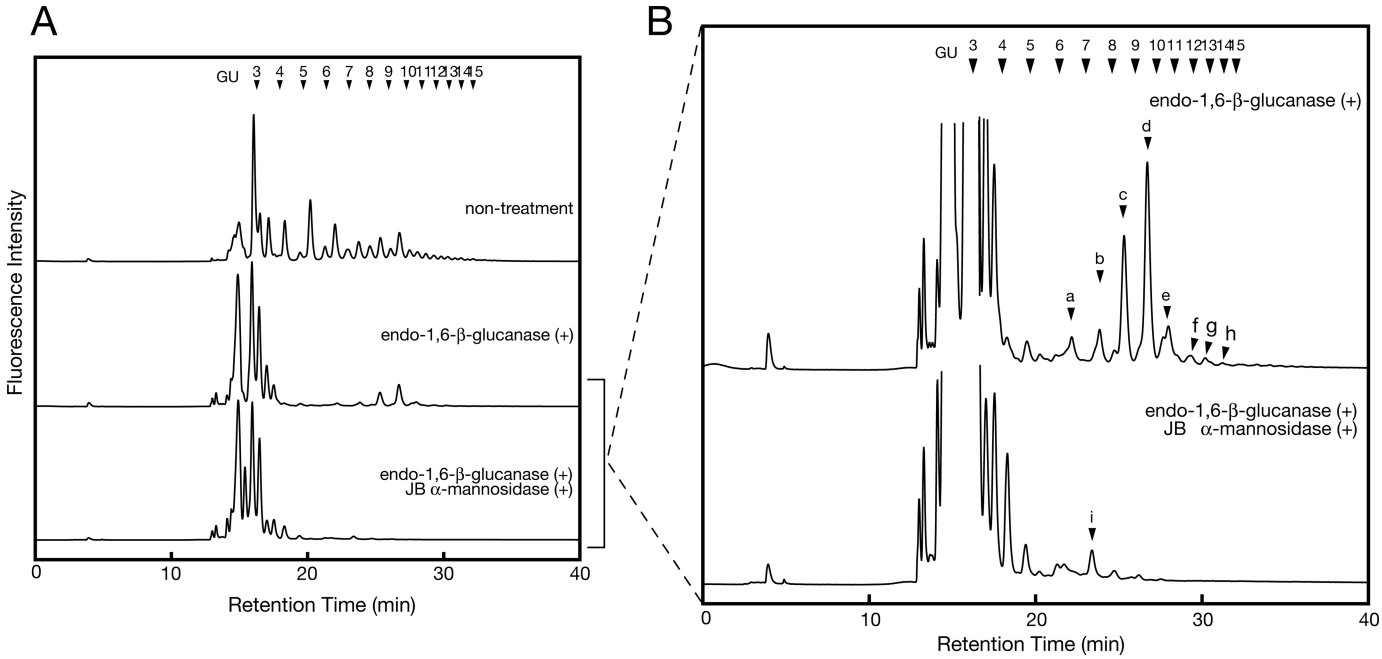

FIGURE 2. **Endo-β-1,6-glucanase treatment of PA-oligosaccharides prepared from wild-type cells.** *A*, size fractionation HPLC profile of glycosidase-treated PA-oligosaccharides isolated from yeast cytosol. Profiles of non-treated control oligosaccharides (*top*), oligosaccharides treated with endo-β-1,6-glucanase (*middle*), and oligosaccharides treated with both endo-β-1,6-glucanase and JB mannosidase (*bottom*) are shown. *B*, magnification of the *middle* and *lower* charts in *A*. *Peaks a–f* indicate *N*-glycan-derived fOSs. The *arrowheads* indicate the elution position of PA-isomaltooligosaccharides (glucose oligomer) for the elution standard.

from β-glucans. To validate this possibility, we first tried to digest these mannosidase resistance peaks with laminarinase (endo-1,3(4)-β-glucanase) or Zymolyase-100T (β-1,3-glucan laminaripentaohydrolase), but they were resistant to these treatments (data not shown). These results suggested that PA-fOSs were not derived from β-1,3-glucans. Enzymes acting on β-1,6-glucans are not commercially available; therefore, we expressed His_6-tagged *Neurospora crassa* endo-1,6-β-glucanase (His_6-Neg1) in *E. coli* (supplemental Fig. S2*A*) and purified it on a nickle affinity column. The enzyme was successfully purified (supplemental Fig. S2*B*), and the specific activity was increased 44-fold with a yield of 11% (supplemental Table S1). We then examined the effect of endo-1,6-β-glucanase treatment on PA-fOSs. It was found that endo-1,6-β-glucanase could remove most of the mannosidase-resistant peaks at the elution position relating to 4–15 GUs (Fig. 2*A*). The peaks at the elution position relating to 3–4 GUs were not digested with endo-1,6-β-glucanase, possibly due to the weak activity of endo-1,6-β-glucanase against length β-glucans (57). It should be noted that the remaining peaks, at positions relating to 6–15 GUs, were sensitive to JB mannosidase after treatment with endo-1,6-β-glucanase (Fig. 2*B*, *peaks a–h*). This strongly suggested that these peaks were derived from *N*-glycans.

Yeast Cells Generate Diverse Forms of GN2 Type fOSs—Having established a method for the isolation of mannosidase-sensitive fOSs from yeast cells, we next tried to identify the oligosaccharide structures responsible for the mannosidase-sensitive peaks (Fig. 2*B*, *peaks a–h*). For this purpose, the molecular weights of the collected peaks a–h were analyzed by MALDI-TOF MS. It was revealed that the molecular weights of the oligosaccharides responsible for peaks a–h are consistent with the theoretical molecular weight of Hex(5–12)HexNAc2-PA, respectively (Table 2). After JB mannosidase digestion, a remaining peak was observed (Fig. 2*B*, *bottom*, *peak i*), and the molecular weight of this peak was consistent with the theoretical molecular weight of $Hex_6HexNAc_2$-PA by MALDI-TOF MS analysis. Through mapping analysis with authentic PA-labeled samples, the structure was determined to be G1M5 that was converted from monoglucosylated forms of fOSs. Taken together, these results revealed that the remaining peaks, relating to around 6–15 GUs after endo-1,6-β-glucanase treatment, were derived from diverse fOS structures.

TABLE 2
MALDI-TOF MS analysis of size-fractionated PA-glycans

Peak	Observed mass (*m/z*)	Ion formation	Composition
a	1351.8	$[M + K]^+$	$Hex_5HexNAc_2$-PA
b	1497.7	$[M + Na]^+$	$Hex_6HexNAc_2$-PA
c	1659.9	$[M + Na]^+$	$Hex_7HexNAc_2$-PA
d	1821.9	$[M + Na]^+$	$Hex_8HexNAc_2$-PA
e	1984.1	$[M + Na]^+$	$Hex_9HexNAc_2$-PA
f	2145.2	$[M + Na]^+$	$Hex_{10}HexNAc_2$-PA
g	2307.0	$[M + Na]^+$	$Hex_{11}HexNAc_2$-PA
h	2469.9	$[M + Na]^+$	$Hex_{12}HexNAc_2$-PA
i	1497.7	$[M + Na]^+$	$Hex_6HexNAc_2$-PA

All N-Glycan-derived fOSs Are Generated from Misfolded Glycoproteins by the Action of the Cytosolic PNGase, Png1p—As shown in Fig. 1, fOSs are generated by two distinct pathways in mammalian cells. One pathway generates fOSs from misfolded glycoproteins in the cytosol by the action of PNGase, and the other pathway generates fOSs from Dol-PP-OS in the lumen of the ER (27). Using metabolic radiolabeling experiments in yeast cells, it was estimated that generation of fOSs by cells lacking Png1p was reduced by 20–30% compared with that of wild-type cells (52). Thus, we next investigated the structure of fOSs in *png1*Δ cells to determine the structure of Png1p-independent

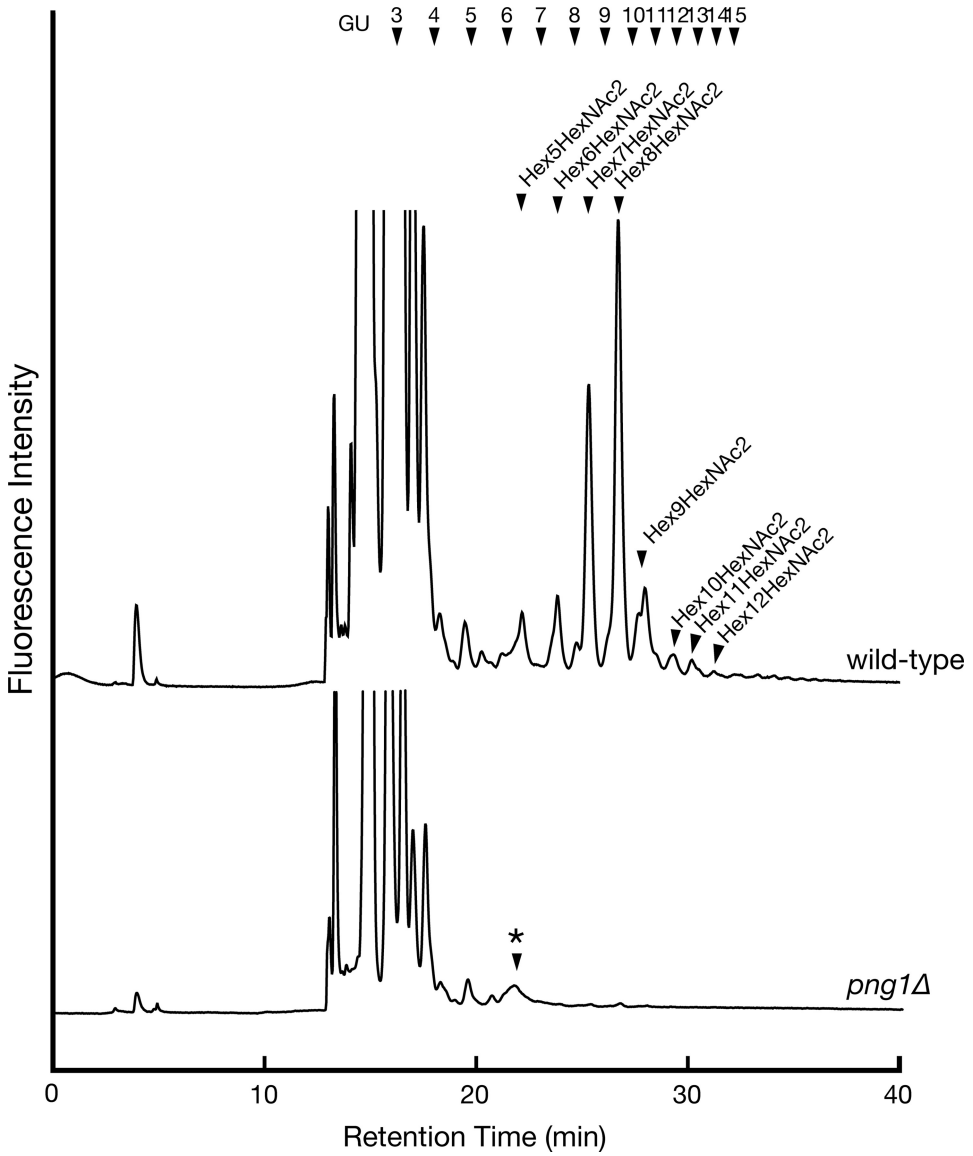

FIGURE 3. **The deletion of *PNG1* causes complete reduction of fOSs generation.** Size fractionation HPLC profile of fOSs derived from wild-type cells (*upper chart*) and *png1*Δ cells (*lower chart*) that were digested with endo-1,6-β-glucanase as described in the legend to Fig. 2. *, nonspecific peak, which is resistant to JB mannosidase treatment.

fOSs. Unexpectedly, fOSs were virtually undetectable in *png1*Δ cells under our experimental conditions (Fig. 3). We therefore concluded that *N*-glycan-derived fOSs in yeast detected by our method were all formed from misfolded proteins by the action of Png1p (see "Discussion").

Yeast Can Create Various Structural Isomers of fOSs—We next asked if the size-fractionated peaks a–h, relating to $Hex_5HexNAc_2$–$Hex_{12}HexNAc_2$, contain diverse structural isomers. To further elucidate the structure of these oligosaccharides, the collected peaks a–h were further separated by reversed-phase HPLC, and their elution positions were compared with those of authentic PA-sugars. Deduced structures based on HPLC mapping were further confirmed by various glycosidase digestions. From this analysis, we successfully identified structures for 14 of 19 major peaks, containing two glycans that have ManNAc in their reducing termini (see Table 3, Footnote *e*). With respect to peak b1, the structure could not be unequivocally identified due to the lack of a standard sample, but it was predicted based on various glycosidase digestions and the fact that this glycan should be derived from larger fOSs already isolated (Table 3; glycosidase digestion data are shown in supplemental Fig. S3). We were also unable to identify the structures relating to peaks g and h, corresponding to the $Hex_{11}HexNAc_2$ and $Hex_{12}HexNAc_2$ forms of fOSs, due to its small amount of material and the lack of suitable authentic samples. Because these glycans were not identical to $Glc_2Man_9GlcNAc_2$-PA and $Glc_3Man_9GlcNAc_2$-PA (data not shown), these fOSs were most likely derived from glycans that are further mannosylated by Golgi-resident mannosyltransferases (see below).

A Part of Misfolded Glycoproteins May Be Recycled between the ER and Golgi, as Evidenced by the Occurrence of Och1p-modified fOSs—As described above, the structures for 5 of 19 major peaks detected could not be determined by HPLC-mapping analysis. Interestingly, all five peaks were converted to $Man_6GlcNAc_2$ by α-1,2-mannosidase treatment, instead of $Man_5GlcNAc$, as would be expected for normal high mannose type glycans in mammalian cells (Fig. 4, *B* and *C*). It is known that yeast *N*-glycan often contains a mannan type polymannose outer chain (Fig. 4*A*) (53–55). The initiation of this outer chain elongation is mediated by a *cis*-Golgi-resident α-1,6-mannosyltransferase, Och1p (Fig. 4*A*) (58–60). We therefore proposed that these glycans bear α-1,6-linked mannose residues modified by Och1p. To confirm this hypothesis, we tried further digestion of the α-1,2-mannosidase-digested product with *Xanthomonas manihotis* α-1,6-mannosidase that is capable of acting on non-branched α-1,6-linked mannose polymers. As expected, the double digestion with α-1,2-mannosidase and α-1,6-mannosidase resulted in a shift in the peaks from M6 to M5 (Fig. 4, *B–E*, size fractionation HPLC charts). These results strongly suggested that these peaks (c3, d2, e1, and f1) have a yeast-specific, Och1p-modified mannose residue.

We next sought to determine the precise structures of Och1p-modified glycans. First, to obtain authentic Och1p-modified glycans, M7A, M7C, M7D, M8B, M8A, M8C, and M9A glycans were reacted with purified Och1p *in vitro*, and the reaction products were designated as M8H, M8I, M8J, M9H, M9I, M9J, and M10H, respectively. The elution positions of

TABLE 3
Free oligosaccharide structures in wild-type and *ams1*Δ cells

Peak	Abbreviations	GU[a]	Structure	Amount (pmol/10 mg proteins)[b,c]	
				WT	*ams1Δ*
f1	M10G[d]	4.79	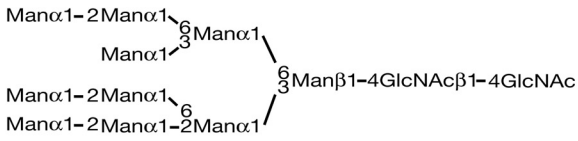	2.6	7.7
f2	M10H	5.79	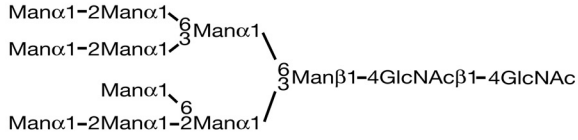	0.4	0.6
f3	G1M9A	6.71	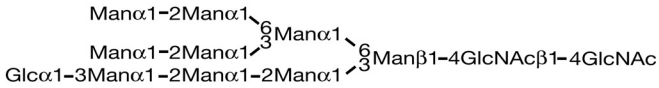	5.0	3.1
e1	M9H	5.31	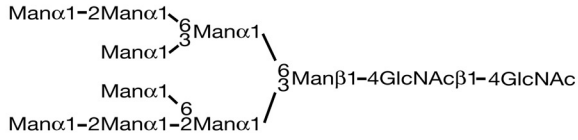	31.0	66.6
e2	M9A	5.80	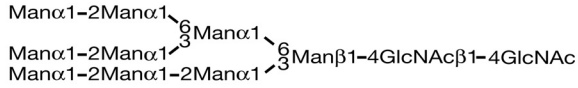	5.1	4.5
e3	G1M8B	6.16	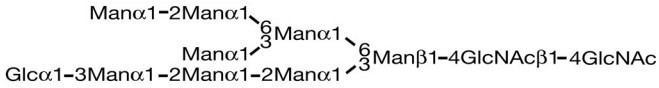	20.2	45.5
e4	G1M8C	7.95	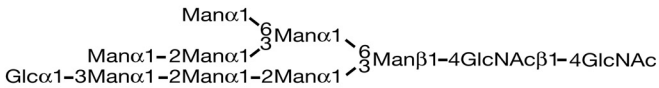	0.7	N. D.
d1	M8B[e]	5.32	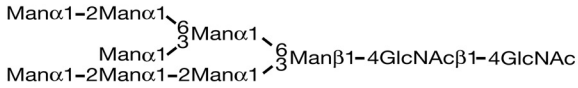	198.0	278.0
d2	M8I	6.05	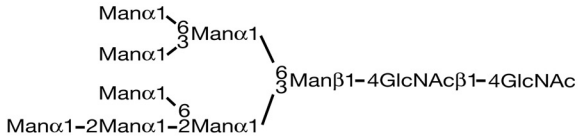	25.7	51.1
d3	M8C	6.67	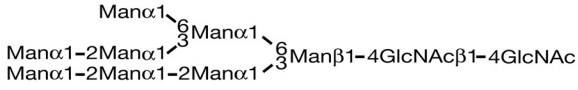	0.9	N. D.
d4	G1M7C	7.22	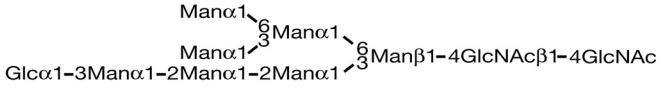	6.4	N. D.

these authentic Och1p-modified glycans were compared with the peaks, c3, d2, e1, and f2, by reversed-phase HPLC. From this analysis, together with analysis by various mannosidase digestions, we identified the precise structures of c3, d2, e1 and f2 as Och1p-modified glycans (Table 3). With respect to f1, designated M10G, we could not determine the precise structure

TABLE 3—*continued*

Peak	Abbreviations	GU[a]	Structure	Amount (pmol/10 mg proteins)[b,c] WT	*ams1Δ*
c1	M7A	5.70	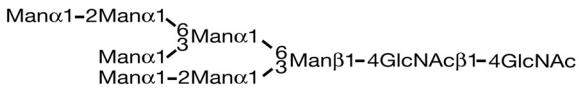	6.7	N. D.
c2	M7C[e]	6.04	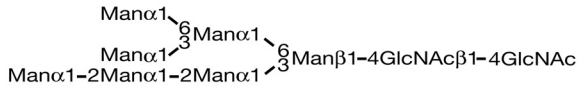	93.9	140.0
c3	M7H	6.41	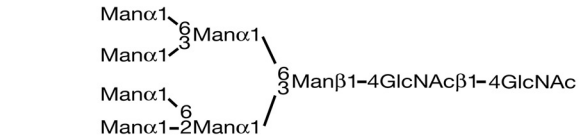	3.4	N. D.
b1	M6[d]	5.99	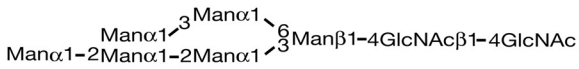	5.5	N. D.
b2	M6B	6.33	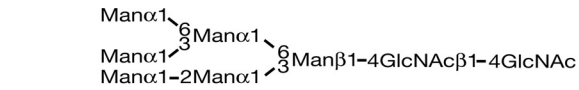	8.0	N. D.
a1	M5A	7.10	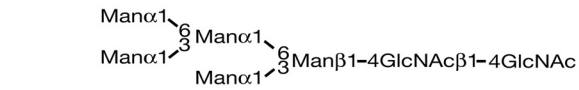	1.7	N. D.

[a] Glucose unit of each PA-labeled oligosaccharide was determined as described under "Experimental Procedures."
[b] Each fOS amount was based on the peak area of each peak with PA-Glc_6 in the PA-glucose oligomer (TaKaRa; 2 pmol/μl) as a reference.
[c] Protein concentration of cell lysates was measured by a BCA assay as described under "Experimental Procedures." N.D., not detected.
[d] Predicted structures of M10G and M6, based on MALDI-TOF MS and various glycosidase digestion analysis.
[e] Amount of M8B/M7C was expressed as a combined sum of M8B/M7C glycans that have GlcNAc or ManNAc in their reducing termini. ManNAc residues were generated by epimerization of the *N*-acetyl group of reducing end GlcNAc during reductive amination in the PA-labeling process as reported previously (45).

because the authentic sample was unavailable; however, based on the results of various glycosidase digestions as well as structure information of other fOSs determined, the structure was predicted as shown in Table 3. This unusual structure (*i.e.* α-1,2-mannose attached to Och1p-modified mannose) has been reported previously (53). The fact that these glycans are modified by Golgi-resident enzymes clearly indicated that at least a part of the misfolded glycoproteins had been recycled between the ER and the Golgi before being exported out of the lumen for degradation.

fOSs Are Processed by Cytosol/Vacuole α-Mannosidase, Ams1p, in the Cytosol—The sole catabolic α-mannosidase in yeast, Ams1p, and an amino peptidase I, Lap4p, are synthesized in the cytosol and transported to the vacuole via the autophagic pathway and/or the cytoplasm to vacuole targeting pathway (Cvt pathway) (61–64). Lap4p was shown to be active only in the vacuole because it requires vacuolar proteolytic processing (65–67); however, it remains to be determined whether Ams1p requires similar processing to be enzymatically active. Previously, Ams1p was shown to be involved in catabolism of fOSs (52), however, the subcellular site of Ams1p action remains to be determined.

We first examined the expression level of Ams1p in both mid-log and stationary phase using a strain in which the chromosomal *AMS1* locus had been replaced with an HA-tagged *AMS1* gene (YME2028). As shown in Fig. 5*A*, high level expression of Ams1-HA was observed when the cells reached stationary phase. This result was consistent with previous reports (61, 63). We next examined the relative amount of fOSs in these cells at mid-log or stationary phase by size fractionation HPLC. In stationary phase cells, an increase of Hex(5–7)HexNAc2 fOSs was observed compared with mid-log phase cells (Fig. 5, *B* and *C*, *upper panels*). On the other hand, formation of $Hex_5HexNAc_2$ and $Hex_6HexNAc_2$ was completely abolished in both mid-log and stationary phase cultures of *ams1*Δ cells (Fig. 5*B*, *middle*), clearly indicating that Ams1p is the sole enzyme responsible for demannosylation of structures smaller than $Man_7GlcNAc_2$ in yeast. In addition, an apparent increase in the amount of fOSs was observed in stationary phase cultures of *ams1*Δ cells (Fig. 5, *B* and *C*, *middle*). Taken together, these results clearly show that Ams1p is involved in the processing of fOSs, especially at stationary phase.

Having confirmed the critical role of Ams1p in the catabolism of fOSs, we next asked whether Ams1p is capable of proc-

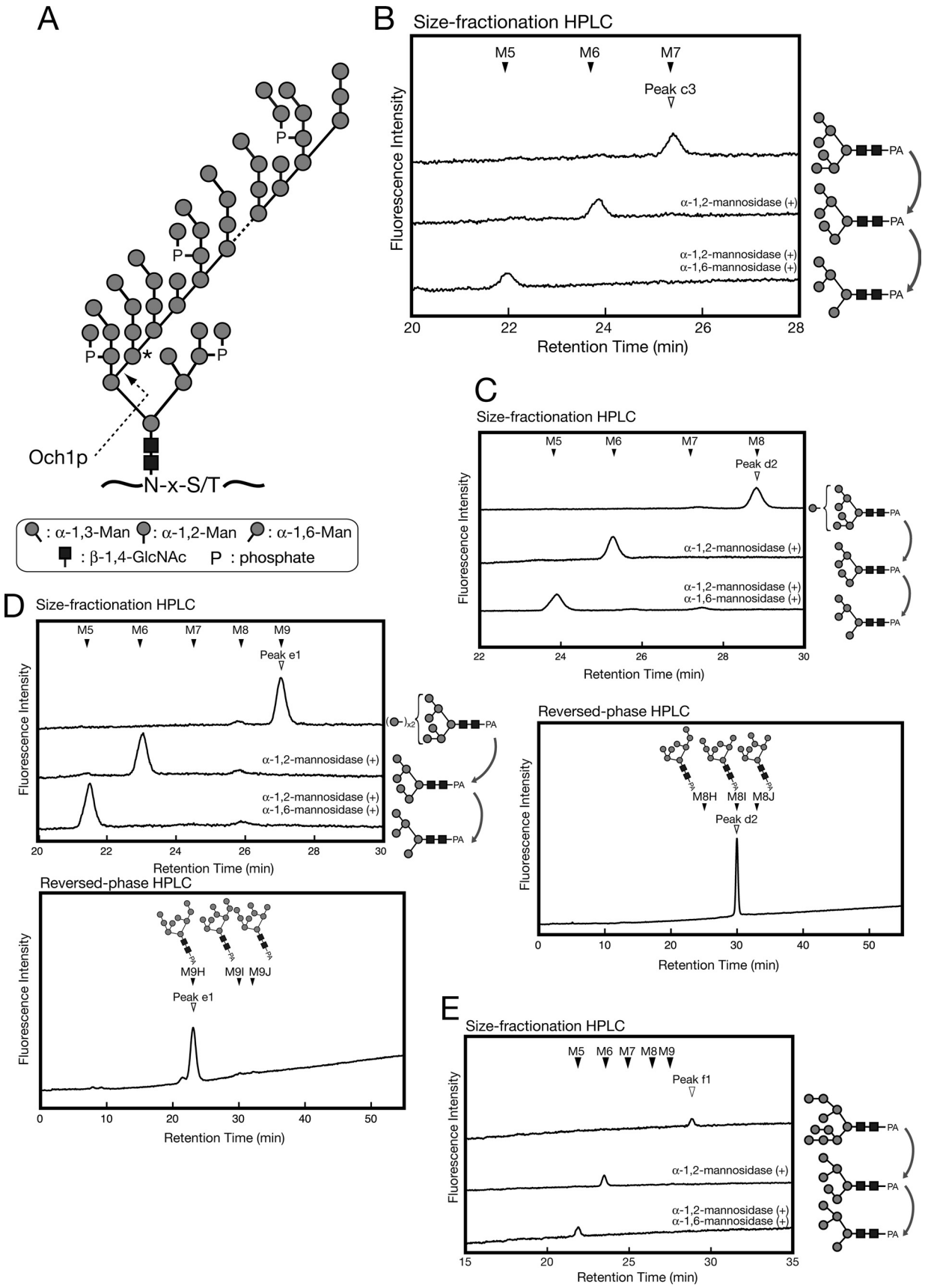

FIGURE 4. **Several fOSs are further modified by Golgi-resident mannosyltransferase, Och1p.** *A*, the structure of the *N*-linked glycan chain in *S. cerevisiae*. The mannose residue added by Och1p is marked by an *asterisk*. *B–E*, unassigned *peaks* (*c3*, *d2*, *e1*, and *f1*) were digested with α-1,2-mannosidase alone or with both α-1,2-mannosidase and α-1,6-mannosidase. *M5–M9* in the *size fractionation HPLC charts* represent elution positions of authentic standards of M5GN2-PA-M9GN2-PA. The elution positions of the authentic standards (M8H, M8I, and M8J) are indicated by *closed arrowheads* (*C* and *D*, *lower chart*).

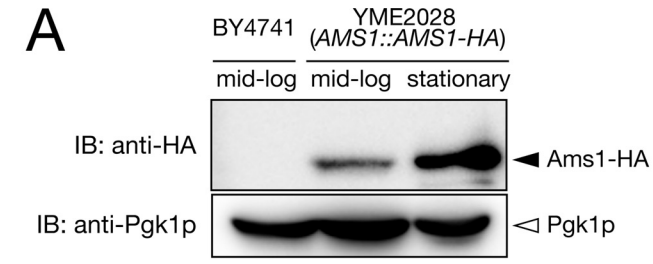
A
BY4741
YME2028
(AMS1::AMS1-HA)
mid-log
mid-log
stationary
IB: anti-HA
Ams1-HA
IB: anti-Pgk1p
Pgk1p

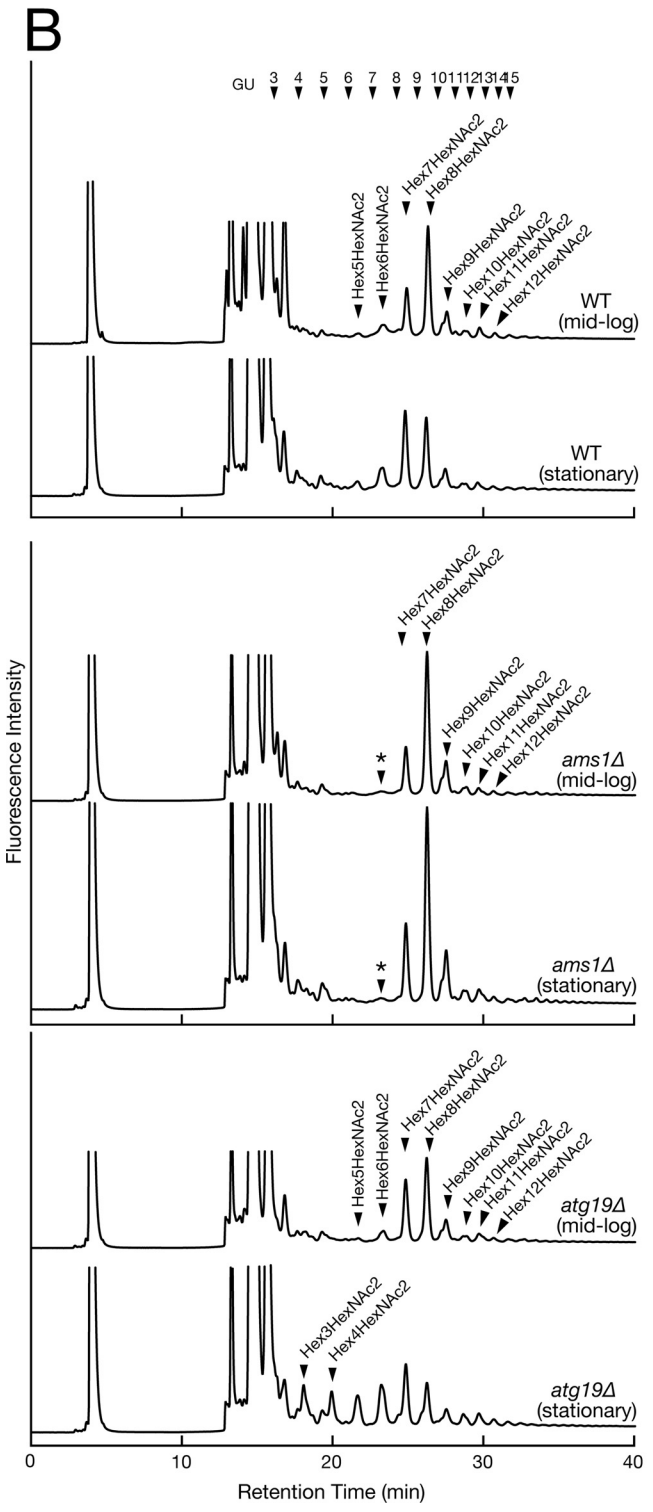
B
GU 3 4 5 6 7 8 9 10 11 12 13 14 15
Hex5HexNAc2
Hex6HexNAc2
Hex7HexNAc2
Hex8HexNAc2
Hex9HexNAc2
Hex10HexNAc2
Hex11HexNAc2
Hex12HexNAc2
WT (mid-log)
WT (stationary)
ams1Δ (mid-log)
ams1Δ (stationary)
atg19Δ (mid-log)
Hex3HexNAc2
Hex4HexNAc2
atg19Δ (stationary)
Fluorescence Intensity
0
10
20
30
40
Retention Time (min)

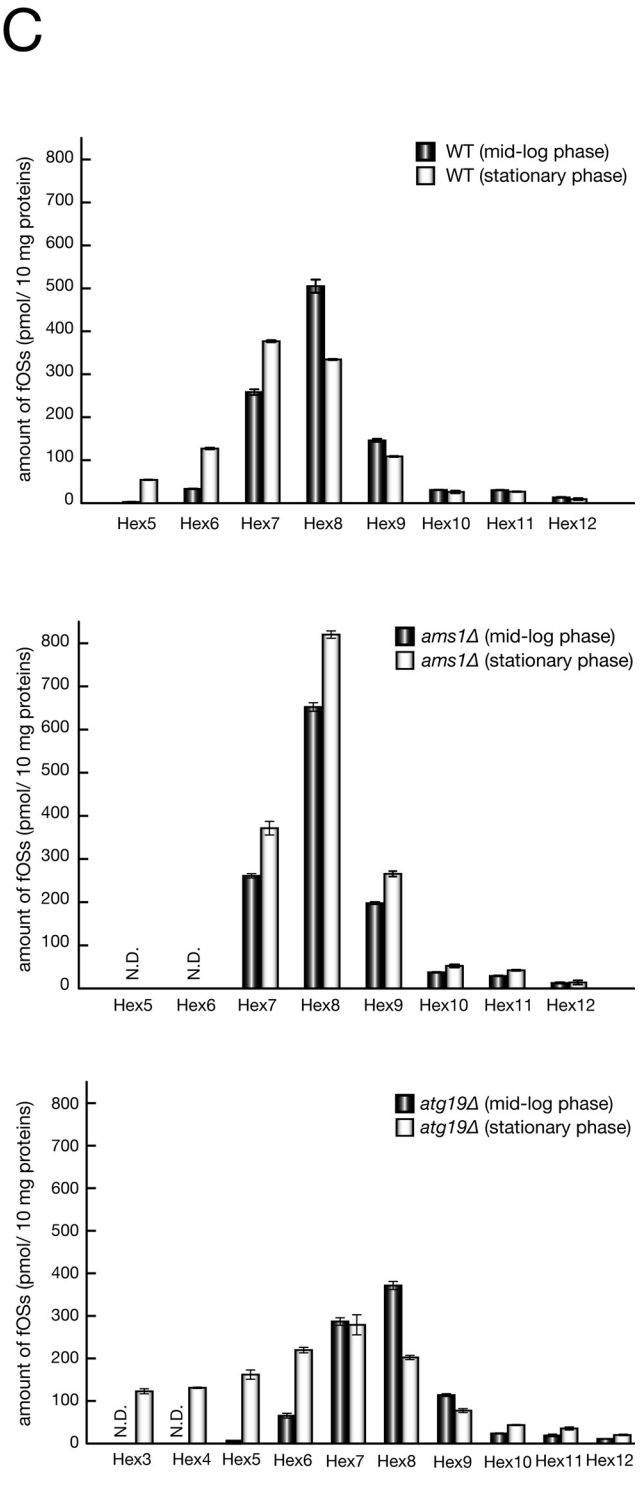
C
WT (mid-log phase)
WT (stationary phase)
amount of fOSs (pmol/ 10 mg proteins)
0
100
200
300
400
500
600
700
800
Hex5
Hex6
Hex7
Hex8
Hex9
Hex10
Hex11
Hex12
ams1Δ (mid-log phase)
ams1Δ (stationary phase)
N.D.
atg19Δ (mid-log phase)
atg19Δ (stationary phase)
Hex3
Hex4

essing fOSs in the cytosol. In these experiments, fOSs were analyzed in *atg19*Δ cells. Atg19p is a receptor specific for the Cvt pathway, and disruption of Atg19p function results in accumulation of Lap4p and Ams1p in the cytosol (68, 69). As shown in Fig. 5*C* (*bottom*), the occurrence of more processed Hex(3–4)HexNAc2 glycans and a significant increase in Hex(5–6)HexNAc2 glycans were evident at stationary phase. This result clearly indicated that Ams1p can be enzymatically active in the cytosol, where it can efficiently degrade fOSs.

*The Structures of fOSs in ams1*Δ *Cells Reflect Those of N-Glycans on Misfolded Glycoproteins Destined for Degradation by ERAD*—Given the fact that Ams1p might be the only cytosolic glycosidase that acts on fOSs and that all fOSs are formed by Png1p under our system, It is strongly suggested that fOSs in *ams1*Δ cells reflect the *N*-glycan structures on misfolded glycoproteins subjected to degradation by ERAD. Thus, we further examined whether the amount and structure of fOSs are altered when *ams1*Δ cells are exposed to ER stress conditions, induced by treatment with DTT or tunicamycin (Tm) (Fig. 6*A*). It is known that Hac1p encodes a transcriptional factor involved in unfolded stress response (unfolded protein response (UPR)) and that *HAC1* mRNA is constitutively transcribed but is not translated (*HAC1*^{u}), due to the presence of an inhibitory intron (70, 71). When yeast cells are exposed to ER stress conditions, activated ER stress sensor, Ire1p, removes the intron from *HAC1*^{u}, and tRNA ligase connects the two exons to generate *HAC1*^{i}. *HAC1*^{i} is then efficiently translated and facilitates transcription of UPR target genes (72–74). We therefore confirmed induction of UPR by formation of the *HAC1*^{i} splicing form (Fig. 6*B*). As shown in Fig. 6*C*, when UPR was activated by DTT, an increased total amount of Hex(8–12)HexNAc2 was observed. On the other hand, the total amount of $Hex_7HexNAc_2$ was unaltered (Fig. 6, *C* (*top* and *middle charts*) and *D*). It should be noted that the total amount of fOSs in Tm-treated *ams1*Δ cells was reduced compared with control cells (Fig. 6, *C* (*top* and *bottom charts*) and *D*). This result is consistent with the fact that Tm can inhibit the biosynthesis of donor substrate (Dol-PP-OS) for *N*-glycosylation (75, 76). To analyze fOS structure under ER stress conditions in more detail, isomeric structures of fOSs were further determined by reversed phase HPLC. As shown in Fig. 6*E*, an increase of M8B, M9H, M9A, and M10G was observed by DTT treatment. In sharp contrast, the total amount of M7C was unchanged. This result indicated that the Htm1p/Yos9p-dependent pathway, which requires M7C glycans as a key structure for recognition, may not play a major role under ER stress conditions.

DISCUSSION

N-Glycosylation is now recognized as one of the most important modification reactions in eukaryotic cells. Explosive progress in glycobiology during the past decade has unveiled most, if not all, of the biosynthetic pathways for *N*-glycans. However, the mechanisms by which *N*-glycans are catabolized in cells are relatively unknown (77). This is especially the case for the metabolism of fOSs. Although the presence of fOSs in various eukaryotes has been detected, the molecular mechanisms behind their formation/degradation have remained largely unknown.

In yeast cells, how fOSs are generated, processed, and degraded remained unclear because of the lack of an established method for the isolation of fOSs. In the current study, we successfully established a method for the isolation of fOSs from the cytosol of yeast cells by eliminating β-1,6-glucans, using purified endo-1,6-β-glucanase (Fig. 2). It remains unclear whether extracellular β-1,6-glucans are made in the secretory pathway or at the cell surface (78). Our results clearly indicated that at least some of the β-1,6-glucan pools can be observed in the cytosol, and this result may help to elucidate the molecular mechanisms of the biosynthetic pathway for β-1,6-glucans. Alternatively, these cytosolic pools of β-1,6-glucan may represent degradation intermediates, although such a degradation process has not, to the best of our knowledge, been described to date.

In higher eukaryotes, it has been reported that there are two types of fOSs: one from misfolded glycoproteins and the other from Dol-PP-OSs (Fig. 1, *A* and *B*) (18, 19, 26, 27). Our data clearly showed that formation of fOSs pooled in the cytosol were exclusively dependent on the activity of Png1p, suggesting that, at least under our experimental conditions, fOSs released from Dol-PP-OSs are not active in yeast. This result was further supported by the observation that no fOS was detected in either mid-log or stationary phase of *ams1*Δ *png1*Δ cells (data not shown). The lack of Png1p-independent fOS release was contrasted by the findings of Chantret *et al.* (52), which indicated the occurrence of Png1p-independent fOSs. This seeming discrepancy most likely comes from the difference in fOS isolation methods. Chantret *et al.* (52) isolated fOSs from whole cell extracts, whereas we isolated fOSs from the cytosolic fraction. The absence of Png1p-independent glycans in the cytosol is consistent with the fact that they are most likely formed in the lumen of the ER (28). How these Png1p-independent fOSs are catabolized remains unclear.

Through our newly established method, we observed that yeast cells generate quite diverse forms of fOSs even in the absence of Ams1p, suggesting that misfolded glycoproteins undergo various types of glycan processing in the lumen prior to retrotranslocation. However, yeast cells do not appear to generate the GN1 form of fOSs, in contrast to higher eukaryotes in which the GN1 form is the major fOS structure (33–35, 40). The lack of the GN1 form of fOSs in yeast cells is consistent with the

FIGURE 5. **Ams1p is involved in fOSs processing in the cytosol.** *A*, expression of Ams1p was significantly elevated at stationary phase. Wild-type (BY4741) and YME2028 (*AMS1*::*AMS1-HA* strain) cells were grown to mid-log or stationary phase. Equal cell numbers were lysed, and total protein extracts were analyzed by immunoblotting using an anti-HA antibody. The immunoblot was subsequently probed with anti-Pgk1p antibody as a protein loading control. *B*, size fractionation HPLC profile of fOSs derived from wild-type, *ams1*Δ, and *atg19*Δ cells. *Hex3–Hex12*, $Hex_3HexNAc_2$–$Hex_{12}HexNAc_2$, respectively. The mass was determined by MALDI-TOF MS analysis. *, nonspecific peak, which is resistant to JB mannosidase treatment. *C*, quantitation of PA-labeled fOSs by size fractionation HPLC. Each *peak* was quantitated with PA-Glc_6, using a PA-glucose oligomer (TaKaRa; 2 pmol/μl) as a reference. *Error bars*, mean ± S.D. from three independent experiments.

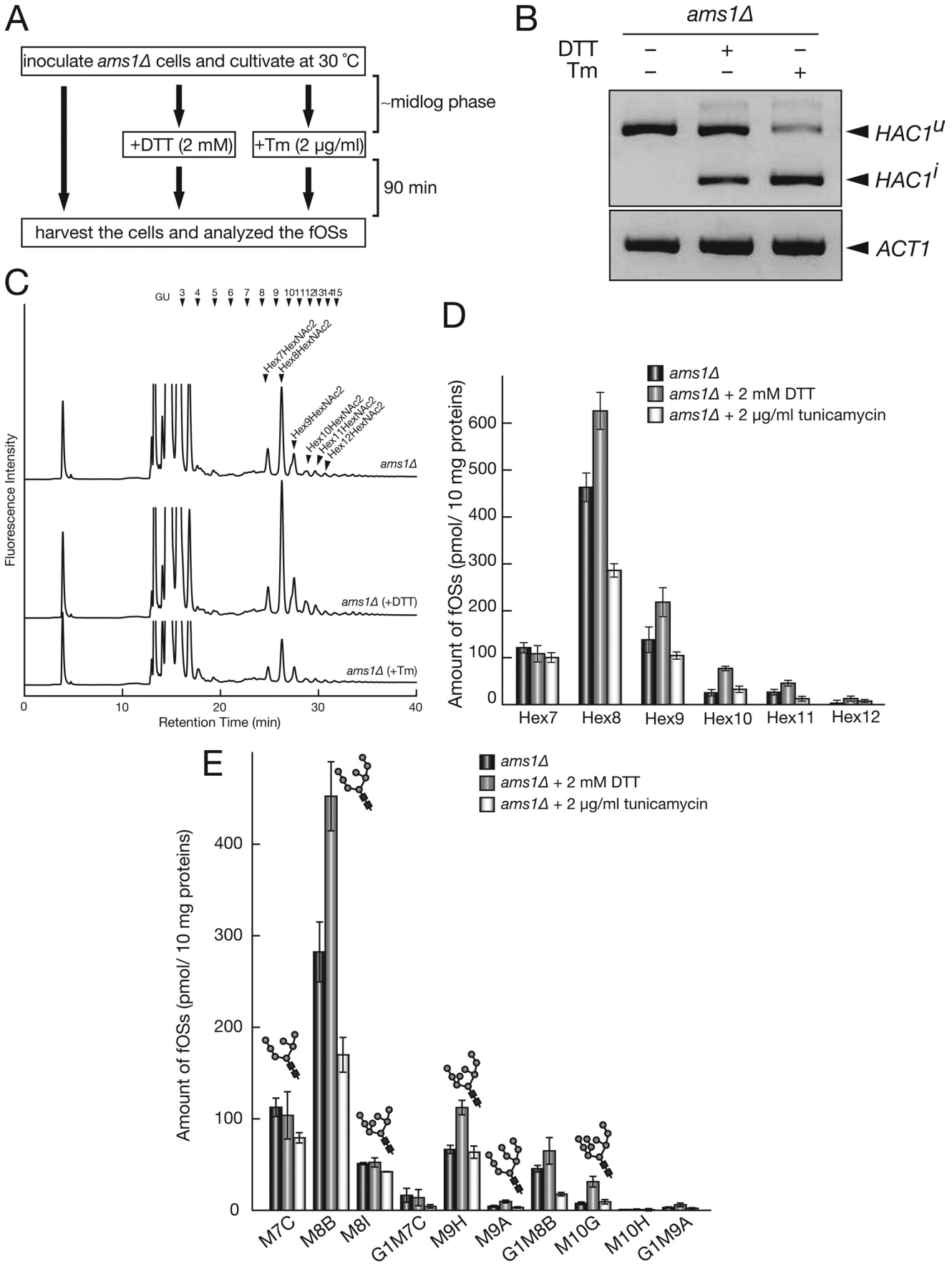
A
inoculate ams1Δ cells and cultivate at 30 °C
~midlog phase
+DTT (2 mM)
+Tm (2 μg/ml)
90 min
harvest the cells and analyzed the fOSs
B
ams1Δ
DTT
Tm
HAC1u
HAC1i
ACT1
C
GU 3 4 5 6 7 8 9 10 11 12 13 14 15
Hex7HexNAc2
Hex8HexNAc2
Hex9HexNAc2
Hex10HexNAc2
Hex11HexNAc2
Hex12HexNAc2
ams1Δ
ams1Δ (+DTT)
ams1Δ (+Tm)
Fluorescence Intensity
Retention Time (min)
D
ams1Δ
ams1Δ + 2 mM DTT
ams1Δ + 2 μg/ml tunicamycin
Amount of fOSs (pmol/ 10 mg proteins)
Hex7
Hex8
Hex9
Hex10
Hex11
Hex12
E
ams1Δ
ams1Δ + 2 mM DTT
ams1Δ + 2 μg/ml tunicamycin
Amount of fOSs (pmol/ 10 mg proteins)
M7C
M8B
M8I
G1M7C
M9H
M9A
G1M8B
M10G
M10H
G1M9A

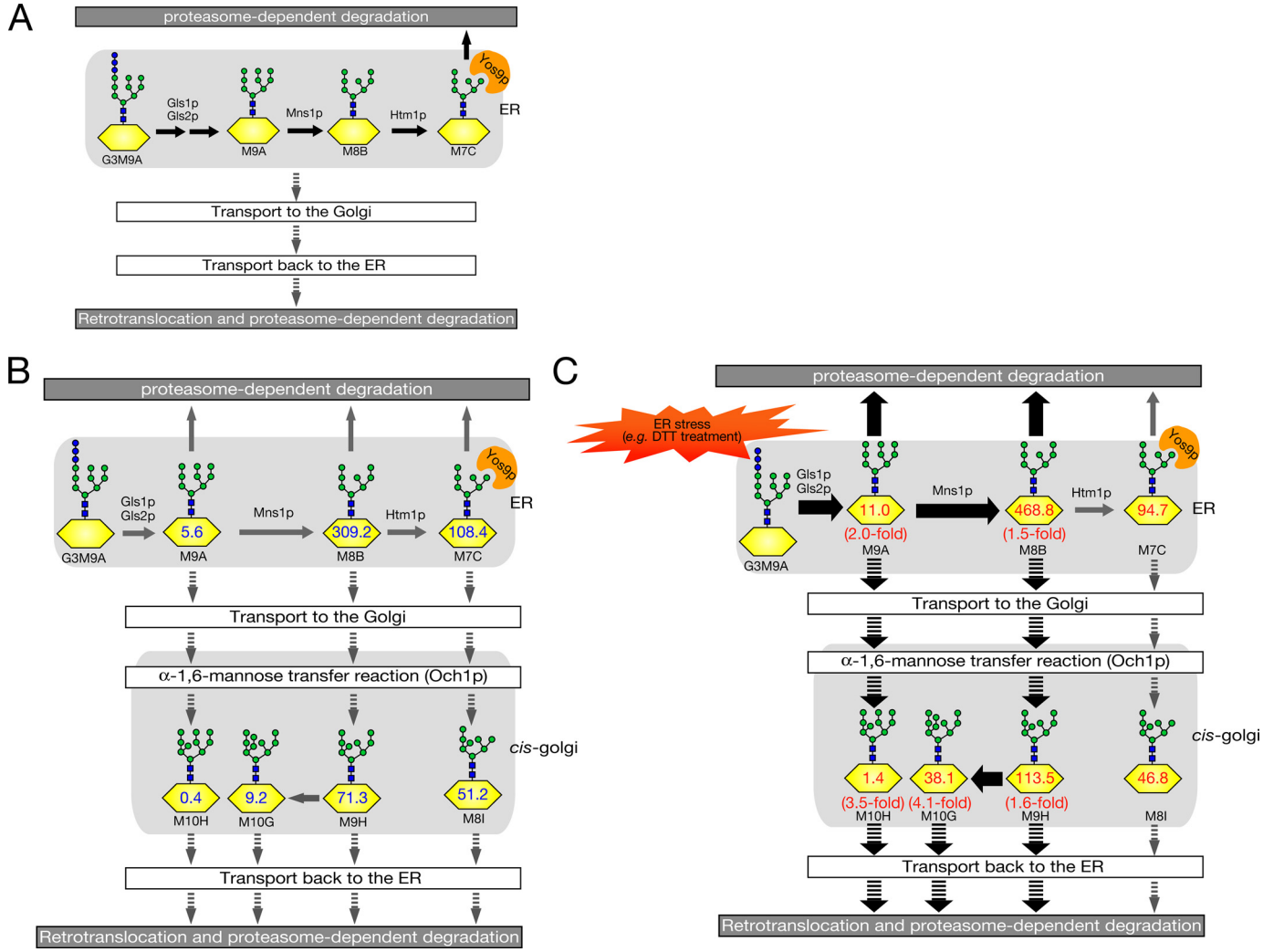

FIGURE 7. **Predicted scheme for overall *N*-glycan processing on misfolded glycoproteins subjected to ERAD.** *A*, a current model for *N*-glycan processing in glycoprotein ERAD (14). *N*-Glycans on misfolded glycoproteins are further trimmed by glucosidases (Gls1p and Gls2p) and mannosidases (Mns1p and Htm1p), which can generate M7C glycan. Yos9p, a lectin-like ERAD component, recognizes the α-1,6-terminal mannose residue of M7C. Several misfolded glycoproteins may traffic between ER and Golgi before their degradation, as depicted by *downward arrows*. *B*, hypothetical scheme of *N*-glycan processing on misfolded glycoproteins, based on our fOS analysis. The *numbers* (pmol/10 mg protein) on *N*-glycans are based on fOSs analysis in *ams1*Δ cells. *C*, when UPR is induced by DTT, yeast cells facilitate the generation of M8B glycans on misfolded proteins and transport misfolded glycoproteins to the Golgi. *Thick arrows* indicate pathways up-regulated by UPR.

fact that the orthologue of endo-β-*N*-acetylglucosaminidase cannot be found in the yeast genome (32). It is interesting to note that the most abundant fOSs in *ams1*Δ yeast cells is M8B. Recently, a couple of studies have elegantly shown that at least some of the glycoprotein ERAD substrates depend on the activity of Htm1p (EDEM orthologue acting as α-mannosidase)/Yos9p (lectin recognizing α-1,6-mannose exposed by Htm1p action) for their efficient retrotranslocation/degradation by the ERAD pathway (Fig. 7*A*) (11, 14, 79). However, at least from the glycan profile of fOSs, it can be assumed that the glycans processed by Htm1p (to form M7C glycan) are relatively minor. One plausible explanation for this observation is that only a specific glycan, among the multiple *N*-glycans on misfolded glycoproteins, may act as a recognition signal for Htm1p/Yos9p-dependent degradation (Fig. 7*B*). This hypothesis is supported by the fact that a specific *N*-glycan on multiple glycosylated misfolded model proteins, CPY* and PrA*, functions as a tag for targeting to the ERAD pathway (17, 80). An alternative possibility is that there may be many *N*-glycosylated substrates that are degraded by the ERAD pathway in an Htm1p-independent manner, as suggested by previous reports (81, 82).

We also found that several forms of fOSs were subjected to yeast-specific glycan modification (Table 3). This modification was found to be mediated by a Golgi-resident α-1,6-mannosyl-

FIGURE 6. **fOSs structures in *ams1*Δ cells reflect *N*-glycan structures on misfolded glycoproteins.** *A*, scheme of ER stress induction. *ams1*Δ cells were inoculated and grown to mid-log phase at 30 °C. Then 2 mM DTT or 2 μg/ml Tm was added to the medium as described previously (86), and cells were further incubated at 30 °C for 90 min. Samples were then collected, and fOSs were analyzed. *B*, reverse transcription-PCR analysis of *HAC1* mRNA splicing. *HAC1*^{u} and *HAC1*^{i} are uninduced and induced *HAC1* by the UPR, respectively. *C*, size fractionation HPLC profile of fOSs derived from *ams1*Δ cells treated with or without UPR-induced reagents. *D*, quantitation of fOSs observed in *C*. *Hex7–Hex12*, $Hex_7HexNAc_2$–$Hex_{12}HexNAc_2$, respectively. *Error bars*, mean ± S.D. from three independent experiments. *E*, quantitation of fOSs separated by reversed phase HPLC. *Error bars*, mean ± S.D. from three independent experiments.

transferase, Och1p, and this Och1p-dependent fOS modification was abolished in *och1*Δ cells.[3] It should be noted that all Och1p-modified fOSs, so far detected, did not accept further elongation of α-1,6-linked mannose on Och1p-modified mannose. Because the poly-α-1,6-mannose structure can be found quite commonly in yeast cell surface *N*-glycoproteins, our result might indicate the presence of an uncharacterized quality control system for misfolded glycoproteins in the Golgi. Such a mechanism might prevent misfolded proteins from proceeding further in the secretory pathway and thereby receiving poly-α-1,6-mannose chains and instead help them to be retrieved to the ER and the ERAD pathway. It has been reported that *C. elegans* also generates fOSs, possibly modified in the Golgi (40), although it remains to be determined whether these Golgi-modified fOSs were from misfolded glycoproteins or, alternatively, from Dol-PP-OS. In sharp contrast, our results clearly demonstrated that Golgi-modified glycans are formed by Png1p and therefore derived from misfolded glycoproteins, which might have traveled from the ER to the Golgi (Fig. 7). This notion is supported by reports that the ER-to-Golgi trafficking of several model misfolded glycoproteins, including CPY*, KHNt, and Gas1*, is important for their efficient degradation by the ERAD pathway (82–85). At this time, the question of whether there is any physiological significance of the modification of misfolded glycoproteins by Och1p remains elusive.

Elevated expression of Ams1p at stationary phase (Fig. 5*A*) was consistent with the observation that the processing of fOSs by Ams1p was more pronounced at stationary phase (Fig. 5*B*, *top*). The biological significance of Ams1p up-regulation at stationary phase remains to be determined.

In *ams1*Δ cells, the generation of M5 and M6 forms of fOSs was abolished completely. This result suggested that processing beyond $Man_7GlcNAc_2$ glycans was generated solely by Ams1p in yeast. Furthermore, the small amount of fOSs observed in wild-type cells, including M8C, G1M8C, and M7H, was not observed in *ams1*Δ cells (Table 3). Thus, these fOSs also seem to be produced by Ams1p. We also showed that *atg19*Δ cells, possessing a defect in Ams1p transport from the cytosol to the vacuole, can process fOSs more efficiently than wild-type cells. This is the first report to unequivocally demonstrate that Ams1p has enzyme activity even without being targeted to the vacuole.

It is noteworthy that under DTT stress, the overall amount of fOSs was increased (*i.e.* indication of the aggravation of overall glycoprotein ERAD), but no change in the amount of M7C was observed (Fig. 6*C*). Further studies will be required to clarify the detailed mechanism by which DTT affects glycoprotein ERAD in yeast. One potential explanation for this observation is that, upon UPR activation (*e.g.* DTT treatment), most of the substrates that undergo ERAD follow the Htm1p/Yos9p-independent pathway (Fig. 7*C*). This hypothesis is consistent with the observation that under the UPR, no up-regulation of Htm1p was observed (86), in sharp contrast to that seen in mammalian cells (87). The possibility remains that a yet uncovered, Yos9p-independent glycan recognition pathway could be activated by the UPR, although there is no experimental evidence to support this hypothesis. Alternatively, under harsh conditions, up-regulation of the *N*-glycan structure-independent ERAD as well as vesicular transport may occur for otherwise Htm1p/Yos9p-dependent substrates to sequester accumulated misfolded (glyco)-proteins. Such interplay between ERAD and vesicular transport has been well documented (88–91). This result might also indicate that the Htm1p/Yos9p-dependent ERAD pathway is easily saturable.

In summary, we have established a method for the quantitative analysis of yeast fOSs and determined its structures using PA labeling followed by HPLC analysis. We also show that fOS analysis in an *ams1*Δ background provides valuable information regarding *N*-glycan processing of misfolded glycoproteins subjected to ERAD. In the future, analysis of fOSs in *ams1*Δ cells, in conjunction with the deletion of various glycoprotein ERAD-related genes (*e.g. MNS1*, *HTM1*, *YOS9*, etc.), will clarify the detailed mechanism and physiological significance of glycan processing of misfolded glycoproteins during the ERAD process.

Acknowledgments—We are grateful to Dr. Markus Aebi (ETH, Zurich, Switzerland) for critical reading of the manuscript. We also thank Dr. Yasunori Chiba (National Institute of Advanced Industrial Science and Technology, Japan) for allowing us to use the Och1p expression system, Dr. Takehiko Yoko-o (AIST, Japan) for providing the YEpU-OCH1 plasmid, and Dr. Ichiro Matsuo (Gunma University, Japan) and Dr. Yukishige Ito (RIKEN Advanced Science Institute, Japan) for providing the $Glc_1Man_9GlcNAc_2$ glycans. We also thank the members of the Glycometabolome Team for fruitful discussions.

REFERENCES

1. Kornfeld, R., and Kornfeld, S. (1985) *Annu. Rev. Biochem.* **54,** 631–664
2. Lehle, L., Strahl, S., and Tanner, W. (2006) *Angew. Chem. Int. Ed. Engl.* **45,** 6802–6818
3. Varki, A. (1993) *Glycobiology* **3,** 97–130
4. Helenius, A., and Aebi, M. (2004) *Annu. Rev. Biochem.* **73,** 1019–1049
5. Ou, W. J., Cameron, P. H., Thomas, D. Y., and Bergeron, J. J. (1993) *Nature* **364,** 771–776
6. Jackson, M. R., Cohen-Doyle, M. F., Peterson, P. A., and Williams, D. B. (1994) *Science* **263,** 384–387
7. Hebert, D. N., Foellmer, B., and Helenius, A. (1996) *EMBO J.* **15,** 2961–2968
8. Xu, X., Azakami, H., and Kato, A. (2004) *FEBS Lett.* **570,** 155–160
9. Caramelo, J. J., and Parodi, A. J. (2008) *J. Biol. Chem.* **283,** 10221–10225
10. Olivari, S., Cali, T., Salo, K. E., Paganetti, P., Ruddock, L. W., and Molinari, M. (2006) *Biochem. Biophys. Res. Commun.* **349,** 1278–1284
11. Clerc, S., Hirsch, C., Oggier, D. M., Deprez, P., Jakob, C., Sommer, T., and Aebi, M. (2009) *J. Cell Biol.* **184,** 159–172
12. Hirao, K., Natsuka, Y., Tamura, T., Wada, I., Morito, D., Natsuka, S., Romero, P., Sleno, B., Tremblay, L. O., Herscovics, A., Nagata, K., and Hosokawa, N. (2006) *J. Biol. Chem.* **281,** 9650–9658
13. Bhamidipati, A., Denic, V., Quan, E. M., and Weissman, J. S. (2005) *Mol. Cell* **19,** 741–751
14. Quan, E. M., Kamiya, Y., Kamiya, D., Denic, V., Weibezahn, J., Kato, K., and Weissman, J. S. (2008) *Mol. Cell* **32,** 870–877
15. Szathmary, R., Bielmann, R., Nita-Lazar, M., Burda, P., and Jakob, C. A. (2005) *Mol. Cell* **19,** 765–775
16. Buschhorn, B. A., Kostova, Z., Medicherla, B., and Wolf, D. H. (2004) *FEBS Lett.* **577,** 422–426
17. Xie, W., Kanehara, K., Sayeed, A., and Ng, D. T. (2009) *Mol. Biol. Cell* **20,**

[3] H. Hirayama and T. Suzuki, unpublished observation.

3317–3329
18. Suzuki, T., Kitajima, K., Emori, Y., Inoue, Y., and Inoue, S. (1997) *Proc. Natl. Acad. Sci. U.S.A.* **94,** 6244–6249
19. Hirsch, C., Blom, D., and Ploegh, H. L. (2003) *EMBO J.* **22,** 1036–1046
20. Kim, I., Ahn, J., Liu, C., Tanabe, K., Apodaca, J., Suzuki, T., and Rao, H. (2006) *J. Cell Biol.* **172,** 211–219
21. Tanabe, K., Lennarz, W. J., and Suzuki, T. (2006) *Methods Enzymol.* **415,** 46–55
22. Kario, E., Tirosh, B., Ploegh, H. L., and Navon, A. (2008) *J. Biol. Chem.* **283,** 244–254
23. Mosse, C. A., Meadows, L., Luckey, C. J., Kittlesen, D. J., Huczko, E. L., Slingluff, C. L., Shabanowitz, J., Hunt, D. F., and Engelhard, V. H. (1998) *J. Exp. Med.* **187,** 37–48
24. Ostankovitch, M., Altrich-Vanlith, M., Robila, V., and Engelhard, V. H. (2009) *J. Immunol.* **182,** 4830–4835
25. Skipper, J. C., Hendrickson, R. C., Gulden, P. H., Brichard, V., Van Pel, A., Chen, Y., Shabanowitz, J., Wolfel, T., Slingluff, C. L., Jr., Boon, T., Hunt, D. F., and Engelhard, V. H. (1996) *J. Exp. Med.* **183,** 527–534
26. Anumula, K. R., and Spiro, R. G. (1983) *J. Biol. Chem.* **258,** 15274–15282
27. Suzuki, T., and Funakoshi, Y. (2006) *Glycoconj. J.* **23,** 291–302
28. Moore, S. E., Bauvy, C., and Codogno, P. (1995) *EMBO J.* **14,** 6034–6042
29. Haga, Y., Totani, K., Ito, Y., and Suzuki, T. (2009) *Glycobiology* **19,** 987–994
30. Kato, T., Hatanaka, K., Mega, T., and Hase, S. (1997) *J. Biochem.* **122,** 1167–1173
31. Suzuki, T., Hara, I., Nakano, M., Shigeta, M., Nakagawa, T., Kondo, A., Funakoshi, Y., and Taniguchi, N. (2006) *Biochem. J.* **400,** 33–41
32. Suzuki, T., Yano, K., Sugimoto, S., Kitajima, K., Lennarz, W. J., Inoue, S., Inoue, Y., and Emori, Y. (2002) *Proc. Natl. Acad. Sci. U.S.A.* **99,** 9691–9696
33. Yanagida, K., Natsuka, S., and Hase, S. (2006) *Glycobiology* **16,** 294–304
34. Iwai, K., Mega, T., and Hase, S. (1999) *J. Biochem.* **125,** 70–74
35. Ohashi, S., Iwai, K., Mega, T., and Hase, S. (1999) *J. Biochem.* **126,** 852–858
36. Saint-Pol, A., Bauvy, C., Codogno, P., and Moore, S. E. (1997) *J. Cell Biol.* **136,** 45–59
37. Saint-Pol, A., Codogno, P., and Moore, S. E. (1999) *J. Biol. Chem.* **274,** 13547–13555
38. Kato, T., Fujita, K., Takeuchi, M., Kobayashi, K., Natsuka, S., Ikura, K., Kumagai, H., and Yamamoto, K. (2002) *Glycobiology* **12,** 581–587
39. Suzuki, T., and Lennarz, W. J. (2003) *Biochem. Biophys. Res. Commun.* **302,** 1–5
40. Kato, T., Kitamura, K., Maeda, M., Kimura, Y., Katayama, T., Ashida, H., and Yamamoto, K. (2007) *J. Biol. Chem.* **282,** 22080–22088
41. Belard, M., Cacan, R., and Verbert, A. (1988) *Biochem. J.* **255,** 235–242
42. Chantret, I., and Moore, S. E. (2008) *Glycobiology* **18,** 210–224
43. Longtine, M. S., McKenzie, A., 3rd, Demarini, D. J., Shah, N. G., Wach, A., Brachat, A., Philippsen, P., and Pringle, J. R. (1998) *Yeast* **14,** 953–961
44. Oyama, S., Yamagata, Y., Abe, K., and Nakajima, T. (2002) *Biosci. Biotechnol. Biochem.* **66,** 1378–1381
45. Suzuki, T., Matsuo, I., Totani, K., Funayama, S., Seino, J., Taniguchi, N., Ito, Y., and Hase, S. (2008) *Anal. Biochem.* **381,** 224–232
46. Kitajima, T., Chiba, Y., and Jigami, Y. (2006) *FEBS J.* **273,** 5074–5085
47. Hase, S. (1994) *Methods Enzymol.* **230,** 225–237
48. Natsuka, S., Adachi, J., Kawaguchi, M., Nakakita, S., Hase, S., Ichikawa, A., and Ikura, K. (2002) *J. Biochem.* **131,** 807–813
49. Hase, S., Hatanaka, K., Ochiai, K., and Shimizu, H. (1992) *Biosci. Biotechnol. Biochem.* **56,** 1676–1677
50. Scrimale, T., Didone, L., de Mesy Bentley, K. L., and Krysan, D. J. (2009) *Mol. Biol. Cell* **20,** 164–175
51. Moore, S. E., and Spiro, R. G. (1994) *J. Biol. Chem.* **269,** 12715–12721
52. Chantret, I., Frénoy, J. P., and Moore, S. E. (2003) *Biochem. J.* **373,** 901–908
53. Ballou, L., Hernandez, L. M., Alvarado, E., and Ballou, C. E. (1990) *Proc. Natl. Acad. Sci. U.S.A.* **87,** 3368–3372
54. Trimble, R. B., and Atkinson, P. H. (1986) *J. Biol. Chem.* **261,** 9815–9824
55. Munro, S. (2001) *FEBS Lett.* **498,** 223–227
56. Kapteyn, J. C., Van Den Ende, H., and Klis, F. M. (1999) *Biochim. Biophys. Acta* **1426,** 373–383
57. Hiura, N., Nakajima, T., and Matsuda, K. (1987) *Agr. Biol. Chem. Tokyo* **51,** 3315–3321
58. Nakayama, K., Nagasu, T., Shimma, Y., Kuromitsu, J., and Jigami, Y. (1992) *EMBO J.* **11,** 2511–2519
59. Nakayama, K., Nakanishi-Shindo, Y., Tanaka, A., Haga-Toda, Y., and Jigami, Y. (1997) *FEBS Lett.* **412,** 547–550
60. Okamoto, M., Yoko-o, T., Miyakawa, T., and Jigami, Y. (2008) *Eukaryot. Cell* **7,** 310–318
61. Hutchins, M. U., and Klionsky, D. J. (2001) *J. Biol. Chem.* **276,** 20491–20498
62. Yoshihisa, T., and Anraku, Y. (1989) *Biochem. Biophys. Res. Commun.* **163,** 908–915
63. Yoshihisa, T., and Anraku, Y. (1990) *J. Biol. Chem.* **265,** 22418–22425
64. Klionsky, D. J., Cueva, R., and Yaver, D. S. (1992) *J. Cell Biol.* **119,** 287–299
65. Cueva, R., García-Alvarez, N., and Suárez-Rendueles, P. (1989) *FEBS Lett.* **259,** 125–129
66. Trumbly, R. J., and Bradley, G. (1983) *J. Bacteriol.* **156,** 36–48
67. Chang, Y. H., and Smith, J. A. (1989) *J. Biol. Chem.* **264,** 6979–6983
68. Shintani, T., Huang, W. P., Stromhaug, P. E., and Klionsky, D. J. (2002) *Dev. Cell* **3,** 825–837
69. Scott, S. V., Guan, J., Hutchins, M. U., Kim, J., and Klionsky, D. J. (2001) *Mol. Cell* **7,** 1131–1141
70. Chapman, R. E., and Walter, P. (1997) *Curr. Biol.* **7,** 850–859
71. Kawahara, T., Yanagi, H., Yura, T., and Mori, K. (1997) *Mol. Biol. Cell* **8,** 1845–1862
72. Nikawa, J., Akiyoshi, M., Hirata, S., and Fukuda, T. (1996) *Nucleic Acids Res.* **24,** 4222–4226
73. Kaufman, R. J. (1999) *Genes Dev.* **13,** 1211–1233
74. Mori, K. (2009) *J. Biochem.* **146,** 743–750
75. Takatsuki, A., Arima, K., and Tamura, G. (1971) *J. Antibiot.* **24,** 215–223
76. Tkacz, J. S., and Lampen, O. (1975) *Biochem. Biophys. Res. Commun.* **65,** 248–257
77. Suzuki, T. (2009) *Trends Glycosci. Glycotechnol.* **21,** 219–227
78. Lesage, G., and Bussey, H. (2006) *Microbiol. Mol. Biol. Rev.* **70,** 317–343
79. Hosokawa, N., Kamiya, Y., Kamiya, D., Kato, K., and Nagata, K. (2009) *J. Biol. Chem.* **284,** 17061–17068
80. Spear, E. D., and Ng, D. T. (2005) *J. Cell Biol.* **169,** 73–82
81. Vashist, S., and Ng, D. T. (2004) *J. Cell Biol.* **165,** 41–52
82. Fujita, M., Yoko-O, T., and Jigami, Y. (2006) *Mol. Biol. Cell* **17,** 834–850
83. Caldwell, S. R., Hill, K. J., and Cooper, A. A. (2001) *J. Biol. Chem.* **276,** 23296–23303
84. Vashist, S., Kim, W., Belden, W. J., Spear, E. D., Barlowe, C., and Ng, D. T. (2001) *J. Cell Biol.* **155,** 355–368
85. Taxis, C., Vogel, F., and Wolf, D. H. (2002) *Mol. Biol. Cell* **13,** 1806–1818
86. Travers, K. J., Patil, C. K., Wodicka, L., Lockhart, D. J., Weissman, J. S., and Walter, P. (2000) *Cell* **101,** 249–258
87. Hosokawa, N., Wada, I., Hasegawa, K., Yorihuzi, T., Tremblay, L. O., Herscovics, A., and Nagata, K. (2001) *EMBO Rep.* **2,** 415–422
88. Spear, E. D., and Ng, D. T. (2003) *Mol. Biol. Cell* **14,** 2756–2767
89. Coughlan, C. M., Walker, J. L., Cochran, J. C., Wittrup, K. D., and Brodsky, J. L. (2004) *J. Biol. Chem.* **279,** 15289–15297
90. Kruse, K. B., Brodsky, J. L., and McCracken, A. A. (2006) *Mol. Biol. Cell* **17,** 203–212
91. Hirayama, H., Fujita, M., Yoko-o, T., and Jigami, Y. (2008) *J. Biochem.* **143,** 555–567